

Polyethylenimine/*N*-Doped Titanium Dioxide Nanoparticle Based Inks for Ink-Jet Printing Applications

F. Loffredo,¹ I. A. Grimaldi,^{1,3} A. De Girolamo Del Mauro,¹ F. Villani,¹ V. Bizzarro,¹ G. Nenna,¹ R. D'Amato,² C. Minarini¹

¹Portici Italian National Agency for New Technologies, Energy, and Sustainable Economic Development (ENEA) Research Center, Piazzale E. Fermi 1, 80055 Portici (Naples), Italy

²Frascati Italian National Agency for New Technologies, Energy, and Sustainable Economic Development (ENEA) Research Center, via E. Fermi 45, 00044 Frascati (Roma), Italy

³Department of Physics, University of Naples "Federico II," via Cintia 1, 80126 Naples, Italy

Received 28 April 2011; accepted 28 April 2011

DOI 10.1002/app.34775

Published online 18 August 2011 in Wiley Online Library (wileyonlinelibrary.com).

ABSTRACT: We developed and characterized inks based on dispersions of *N*-doped titanium dioxide (TiO₂) in polyethylenimine (PEI)/ethanol solutions with chemico-physical properties suitable for the ink-jet printing process. In detail, we prepared suspensions by varying the concentration of the polymeric dispersant to investigate the effect of the dispersant on the time stability and printability of the ink. Moreover, we printed the *N*-doped TiO₂/PEI-based

inks on different substrates and studied as the substrate temperature and the printing parameters influenced the printed product quality. Furthermore, the optical properties and the morphology of the printed films were also investigated. © 2011 Wiley Periodicals, Inc. *J Appl Polym Sci* 122: 3630–3636, 2011

Key words: dispersions; nanoparticles; polyelectrolytes

INTRODUCTION

Titanium dioxide (TiO₂) nanoparticles are commonly employed in applications such as photocatalysts,¹ photovoltaic cells,² batteries,³ photochromic and electrochromic devices,⁴ gas sensors,⁵ and thin-film transistors,⁶ thanks to the strong oxidizing power of the photogenerated holes, the chemical inertness, the high refractive index, the nontoxicity, and last but not least, their low cost. In recent years, particular attention has been devoted to the deposition and patterning of films by TiO₂ solution processing to obtain substrates covered by nanoparticles to be employed as self-cleaning surfaces,⁷ antibacterial agents,⁸ working electrodes for dye-sensitized solar cells,⁹ insulator layers in electronic applications,¹⁰ water and air purification,¹¹ optical applications, and waveguides.¹²

Recently, a new class of functional materials obtained by the chemical modification of TiO₂ nanoparticles has gained increasing interest for photochemical applications; this has allowed the use of modified TiO₂ nanoparticles into the visible light

region of the electromagnetic spectrum.¹³ Particularly, substitutional nitrogen doping was found to be particularly effective in decreasing the band gap of the anatase and, thus, for improving the optical absorption and photocatalytic activity under visible light.¹³ With this remarkable property of *N*-doped TiO₂, the possibility of dispersing these nanoparticles in solution might provide new inputs for the fabrication of scattering layers and in the photocatalytic and photovoltaic research sectors. In addition, time-stable *N*-doped TiO₂-based solutions could further extend the application field up to innovative deposition methods in the ink-jet printing (IJP) technique suitable for the realization of defined patterns.^{14–17}

Although considerable research has been devoted to the synthesis of *N*-doped TiO₂ nanoparticles, to best of our knowledge, no information is available about their deagglomeration and dispersion in solution. However, the indications of the TiO₂ dispersions commonly prepared by means of methods based on the simultaneous synthesis and dispersion of the nanoparticles¹⁸ or on the employment of ultrasonic treatments and polymeric dispersants, such as polyethylenimine (PEI),¹⁹ phosphate-based electrolytes,²⁰ poly(vinyl alcohol),²¹ or poly(acrylic acid),²² are not completely strengthened, and with regard to the preparation method, authors of related studies have reported the difficulty of preparing long time-stable dispersions with small aggregates.^{23–25}

In this work, the synthesis of nitrogen-doped TiO₂ nanoparticles by laser pyrolysis is reported, and a

Correspondence to: F. Loffredo (fausta.loffredo@enea.it).

Contract grant sponsor: Tecnologie per Sistemi di Visualizzazione di Immagini (TECVIM) project, financed by the Ministero dell'Università e della Ricerca; contract grant number: DM 20160.

method for dispersing the nanocomposite is disclosed. The chosen method for preparing the *N*-doped TiO₂ solution rested on the employment of PEI as a polyelectrolyte dispersant, and its influence on the nanodispersion time stability was investigated. In particular, we aimed the preparation of the suspension of *N*-doped TiO₂ nanoparticles at obtaining a material with suitable chemico-physical and time-stability properties to be dispensed by means of the IJP technique, avoiding nozzle clogging, the presence of satellite drops, and deviation of jet direction. For this purpose, suspensions at different polymer concentrations were prepared, and their chemical and physical properties were analyzed. Moreover, the TiO₂/PEI inks were printed on quartz and silicon substrates, and a study of the optimization of the printing parameters (amplitude and duration of the ejecting pulse, drop emission frequency, printhead speed, and substrate temperature) was performed. The morphology and the optical properties of the films were also investigated.

EXPERIMENTAL

Nitrogen-doped TiO₂ nanopowders (indicated in the following text as TiO₂) were synthesized by CO₂ laser pyrolysis with Ti(OPr)₄ as a liquid precursor and NH₃ as a sensitizer. After synthesis, a thermal treatment at 480°C for 4 h was carried out to eliminate the carbon contamination. The X-ray diffraction analysis showed that the TiO₂ nanoparticles were a mixture of two crystalline phases, anatase and rutile.

Linear PEI (Polyscience, weight-average molecular weight = 120,000, Polysciences Inc. Warrington, PA), with the molecular formula (C₂H₅N)_{*x*}, contained all secondary amines. Ethanol (EtOH; Aldrich) was used exactly as supplied.

In this work, three solutions were prepared by the dissolution of different amounts of PEI (5, 10, and 20 mg) in 20 mL of EtOH. For each PEI concentration (0.03, 0.06, and 0.12 wt %), the TiO₂ suspension was prepared by the dispersion of the inorganic nanoparticles (10 mg) in the PEI/EtOH solution (20 mL). All of the suspensions were well dispersed by processing in an ultrasonic bath for 5 min at ambient temperature (*T*_{amb}).

The TiO₂/PEI/EtOH inks were characterized by dynamic laser scattering (DLS) analysis with an HPPS 3.1 system from Malvern Instruments (Worcestershire, UK) at different aging times to evaluate the size distribution and time stability of the TiO₂ aggregates in the suspensions.

The zeta potential (ζ) of each suspension was acquired by means of a laser Doppler electrophoresis ζ analyzer (Malvern Instruments Zetasizer, NanoSeriesZS).

The pH measurements of the samples were performed with an HI9025 microcomputer pH meter

analyzer (Hanna Instruments, Villafranca Padovana, Padova, Italy).

For the evaluation of the surface tension of the prepared dispersions, a Dataphysics OCA 20 system (Filderstadt, Germany) was employed by the pendant drop method. These measurements were performed in clean room at 21°C and a relative humidity of 50% and were repeated five times for each sample.

We evaluated the viscosity–density product by means of an AND SV-10 (A&D Company, Tokyo, Japan) vibroviscometer by introducing sensor plates into the PEI solutions and TiO₂/PEI suspensions at 25°C and working at a low frequency (30 Hz) and amplitude of less than 1 mm. This working condition implied little load to the sample and prevented a temperature rise or damage. To obtain the corresponding absolute viscosity, the density of samples was measured with the samples kept at 25°C. Preliminary printing tests of the TiO₂ suspensions were performed with Aurel customized drop-on-demand inkjet equipment (Aurel S.p.A., Modigliana, Italy) with a single-nozzle Microdrop printhead (Microdrop Technologies GmbH, Norderstedt, Germany). A piezoelectric dispenser head with a 50- μ m nozzle diameter, corresponding to a droplet diameter in flight of about 55 μ m and a 90-pL drop volume, was used. A stroboscopic camera system provided the visual control to adjust the pulse voltage and duration of the piezoelectric actuator to obtain the stable droplet condition, which was realized without satellite drops and filaments and with no deflected ejection direction. This condition was achieved by the application of a 40 μ s long 90-V pulse for all of the investigated inks.

Sequences of overlapped single drops to form lines and surfaces were printed on quartz and silicon substrates at different temperatures [*T*_{amb} and temperature (*T*) = 50°C]. The prints on silicon substrate were carried out at different drop emission frequencies (from 5 to 100 Hz) and drop overlapping degrees (from 50 to 80%) to define the conditions for obtaining the optimized printing quality at a fixed substrate temperature. The prints on quartz substrate were performed with a drop emission frequency and a drop overlapping degree equal to 10 Hz and 50%, respectively.

Optical micrograph and scanning electronic microscopy (SEM; LEO 1530, Carl Zeiss S.p.A., Peabody, MA) analyses were carried out to investigate the morphology of the TiO₂ nanoparticles and nanocomposites printed on silicon substrates.

TiO₂/PEI composites printed on quartz substrate at a 10-Hz drop emission frequency and a 0.5 mm/s printhead speed were optically characterized with ultraviolet–visible (UV–vis) transmittance and reflectance spectra by means of a Lambda 900 PerkinElmer spectrophotometer (Waltman, MA).

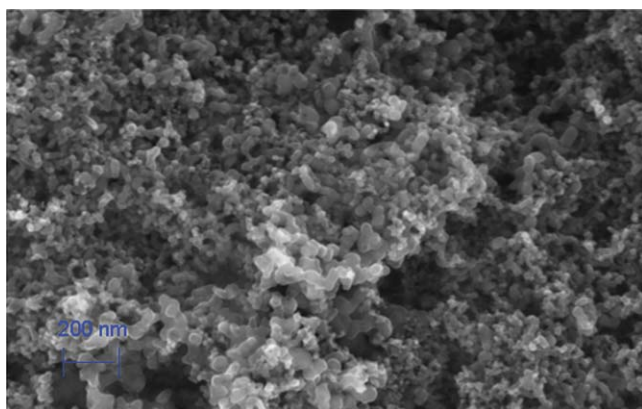


Figure 1 SEM image of *N*-doped TiO₂ nanoparticles. [Color figure can be viewed in the online issue, which is available at wileyonlinelibrary.com.]

RESULTS AND DISCUSSION

The preparation of suitable inks for IJP applications requires some operative phases. After selecting the functional component, the main critical factor is the identification of suitable solvents and additives to obtain good printability of the ink. As far as the solvent is concerned, it should have the right chemical compatibility with both the printhead and the substrate and a useful boiling temperature, viscosity, and surface tension to provide a good wettability of the nozzle and the ink/substrate system and to achieve stable drop conditions. An additive could be used to further improve the chemico-physical properties, the dispersion degree of the functional component, and the time stability.

We employed a homemade nitrogen-doped TiO₂ powder synthesized by laser pyrolysis as a functional material and investigated the nanoparticle morphology by means of SEM analysis. In Figure 1, the SEM image of the sample prepared by the drop casting of a TiO₂/EtOH solution on heated silicon substrate is shown. The nanoparticle average diameter was estimated to be about 15–20 nm.

Moreover, the dispersed nanoparticle powder in EtOH was optically characterized, and the UV–vis absorbance spectrum is illustrated in Figure 2. The absorption band observable in the 250–450-nm wavelength range was due to the *N*-doping, which was responsible for the vivid yellow color of the powder.^{19,26}

It is well known that the TiO₂ nanoparticle surface is generally characterized by the presence of TiOH groups with amphoteric properties that induce an acid–base behavior, depending on the environment pH. In particular, recent studies have shown that the surface of *N*-doped TiO₂ is strongly acidic.²⁷ The choice of employing PEI as the dispersant of our nanoparticles arose just from these considerations.

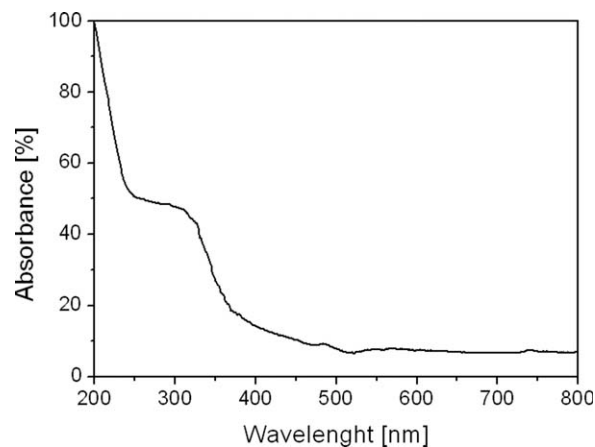


Figure 2 UV–vis transmission spectrum of the dispersed *N*-doped TiO₂ powder in EtOH.

Indeed, this polymer had basic properties because of the presence of ionizable amine groups in the chain.

Because the polyelectrolyte concentration influences the behavior of the colloidal suspension producing stabilization or flocculation,^{28–30} after selecting PEI, we analyzed suspensions at different PEI concentrations. To test the effect of PEI as a cationic polyelectrolyte dispersant on the suspension time stability, we prepared different inks by adding TiO₂ nanoparticles in three PEI/EtOH solutions obtained with different PEI concentrations: 0.03, 0.06, and 0.12 wt %.

The so-prepared suspensions were characterized in terms of size and time stability of the TiO₂ aggregates. The DLS analysis performed at different aging times allowed us to determine the nanoaggregate average size, and the values obtained for all of the TiO₂/PEI/EtOH inks in the time range 0–300 min are reported in Figure 3. The DLS data suggest that

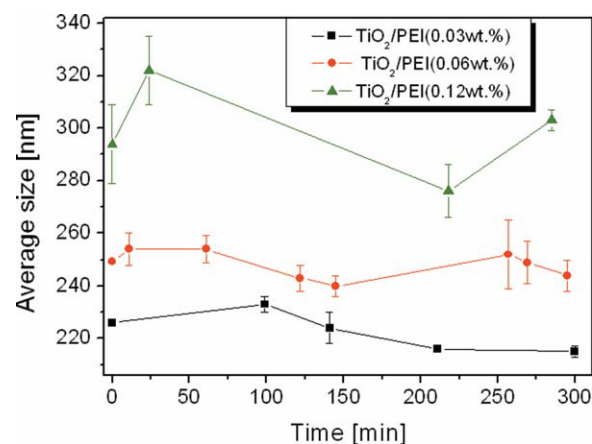


Figure 3 Average size of *N*-doped TiO₂ aggregates for TiO₂/PEI suspensions at different PEI concentrations measured by DLS analysis in the time range from 0 to 300 min. [Color figure can be viewed in the online issue, which is available at wileyonlinelibrary.com.]

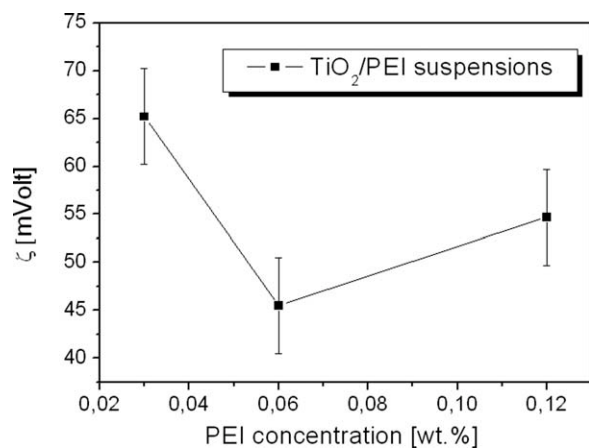


Figure 4 ζ values of the TiO₂/PEI inks at different PEI concentrations.

the analyzed TiO₂/PEI suspensions were well dispersed and were characterized by submicrometer TiO₂ aggregates. Moreover, the aggregate dimensions remained constant in the examined time range; this indicated a suitable ink time stability. A slight phenomena of sedimentation was observed only after 1 day, and the amount of sediments resulting was negligible with respect to the total concentration (<0.06 wt %) and did not compromise its employment as ink. On the contrary, the TiO₂/EtOH suspensions without PEI showed an evident, macroscopic, almost complete sedimentation during the investigated time range. The improvement of the dispersion degree and the time stability of the suspension with the introduction of PEI was basically due to the good chemical affinity of this dispersant with the metallic oxides, which introduced both electrostatic (related to the repulsion of the partially protonated amine groups) and steric (relative to the presence of a chain with high molecular weight) interactions. As a result, these interactions intensified the repulsion among the nanoparticles.¹⁹ Moreover, a small increment of the nanoaggregate dimension was observable as the PEI concentration increased (Fig. 3). This effect could have been due to an excessive dispersant content and may have been accounted for by the double-layer adsorption theory.²⁷ A two-layer structure of adsorbent was formed when excess dispersant molecules were adsorbed onto the ordered molecule surface of TiO₂ particles. The outer layer of dispersant molecules had a tendency to pull the inner layer of the molecules out by electrostatic attraction. As result, the stabilizing ability of the dispersant was impaired as a whole.

To further deepen the prepared dispersion stability, we performed measurements of ζ , a property that reflects the intensity of the repulsive force among the particles in suspension and is, therefore,

correlated to its stability. The ζ data of the TiO₂/PEI inks at different PEI concentrations are shown in Figure 4, and their positive values for the TiO₂/PEI suspensions were attributable to the adsorption of the positively charged PEI on the TiO₂ particles. For all of the analyzed samples, the ζ values are in the range 65–45 mV, higher than 30 mV, the reference value to ensure an electrostatic stabilization and time stability of the suspensions, a crucial condition for obtaining processable inks by means of the IJP technique. The higher potential value associated with TiO₂/PEI (0.03 wt %) could be attributed to several factors, including a lower pH, which implied a higher charge on the PEI molecules. To verify the presence of this effect, pH measurements were performed as a function of the PEI concentration, and the results are shown in Figure 5. The pH values of TiO₂/EtOH, pure EtOH, and PEI/EtOH solutions are also reported as references. The presence of the basic PEI polymer increased the pH value up to 7.5 and ensured the ink-printhead compatibility for the low chemical aggression by neutral pH inks. In particular, the TiO₂/PEI (0.03 wt %) suspension had the lowest pH among the TiO₂/PEI/EtOH inks. Moreover, for the obtained pH values, we expected that the PEI molecules were highly charged and, thus, had an extended conformation. Consequently, the polyelectrolyte could be efficiently adsorbed on the particle surface in flat conformation.¹⁹

Other parameters to be investigated to define the employment of the suspensions as inks were the viscosity and the surface tension. The rheological analysis provided a mean value of the viscosity equal to 1.22 ± 0.05 mPa s for all of the suspensions. This result was justifiable because the prepared solutions were highly dilute and the polymeric molecular

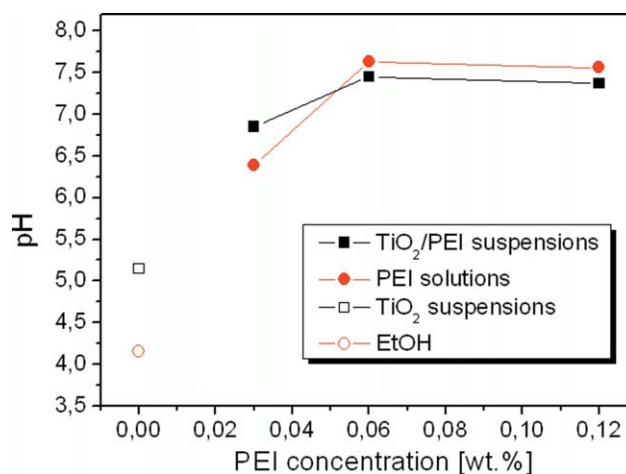


Figure 5 pH measurements of TiO₂/PEI inks and PEI solutions at different PEI concentrations. As references, the pH values of TiO₂/EtOH and pure EtOH are reported. [Color figure can be viewed in the online issue, which is available at [wileyonlinelibrary.com](http://www.interscience.wiley.com).]

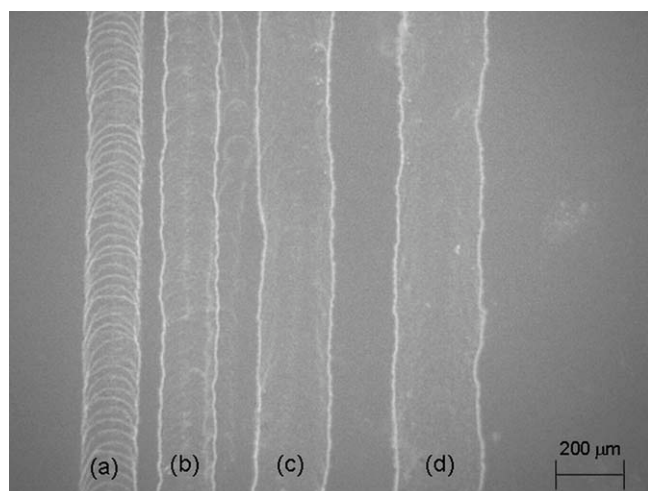


Figure 6 SEM images of TiO₂/PEI (0.03 wt %) printed at $T = 50^{\circ}\text{C}$ and at different drop emission frequencies: (a) 20, (b) 50, (c) 75, and (d) 100 Hz.

weight was low. Also, the surface tension was slightly influenced by the polymer concentration. Precisely, the mean value of this parameter was 32.0 ± 0.4 mN/m, which was included in the in the printhead working range (20–70 mN/m).

The results of the performed chemophysical analyses on the prepared inks demonstrated that the TiO₂/PEI suspensions had suitable properties for IJP applications. Anyway, we chose to investigate the TiO₂/PEI (0.03 wt %) and TiO₂/PEI (0.12 wt %) inks for performing printing tests. The droplet ejecting parameters (pulse voltage and duration) were the same for both inks, and this was consistent with the negligible differences observed in the viscosity and surface tension parameters of the inks.

The effects of the substrate temperature, drop emission frequency, and drop overlapping degree on the line morphology printed on a silicon

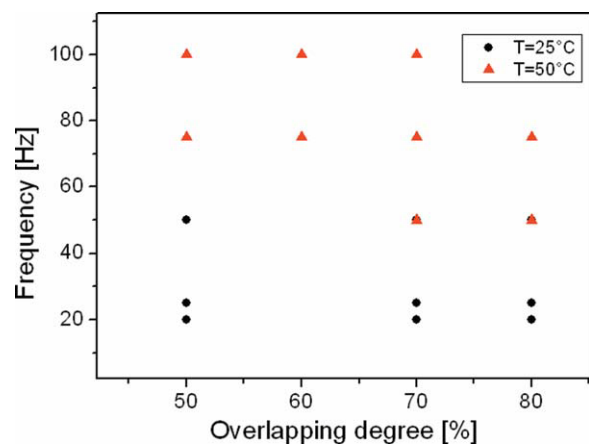


Figure 7 Experimental printing parameters related to the uniform line conditions obtained at (●) T_{amb} and (▲) $T = 50^{\circ}\text{C}$. [Color figure can be viewed in the online issue, which is available at wileyonlinelibrary.com.]

substrate were investigated by means of optical micrographs and SEM images. In Figures 6 is reported, as example, the SEM image of TiO₂/PEI (0.03 wt %) lines printed with different printing parameters. Similar behaviors were observed for the other ink. The morphology changes from stacked coins to a uniform line with changing drop emission frequency and overlapping degree at a fixed substrate temperature (T_{amb} or $T = 50^{\circ}\text{C}$). In addition, the droplet diameter decreased as the substrate temperature increased because the solvent evaporation at $T = 50^{\circ}\text{C}$ was faster, and drops were pinned on the substrate. In the light of these observations, an analysis of the definition of the uniform line condition was needed for each temperature. In Figure 7, the experimental value couples (drop emission frequency, overlapping degree) useful to realize the uniform line conditions for each temperature are reported. As expected and in agreement with analog studies reported in the literature about other materials,³¹ at higher temperatures, the good profile was found at a higher frequency and lower spacing with respect to T_{amb} .

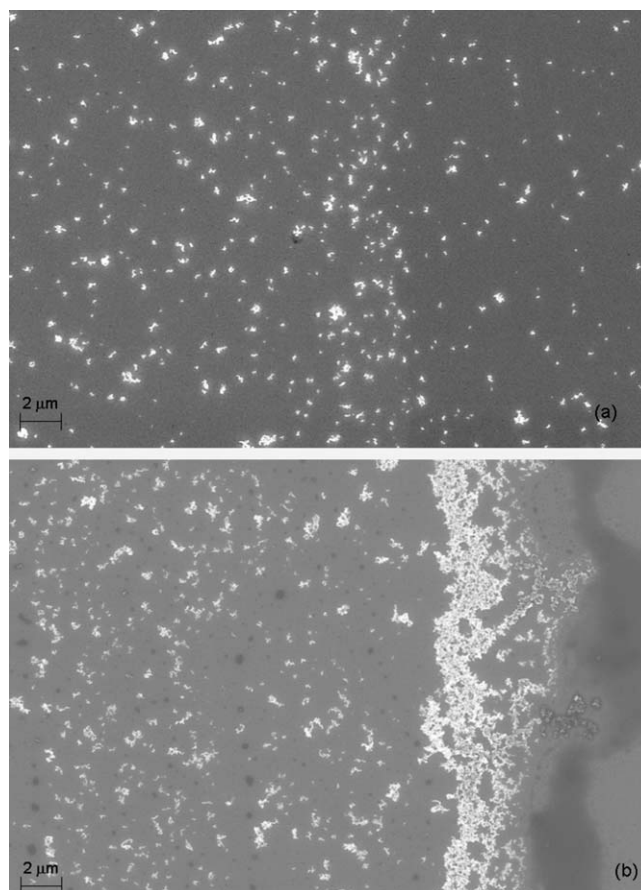


Figure 8 SEM images of TiO₂/PEI (0.03 wt %) printed with an 80% drop overlapping degree at (a) T_{amb} and (b) $T = 50^{\circ}\text{C}$.

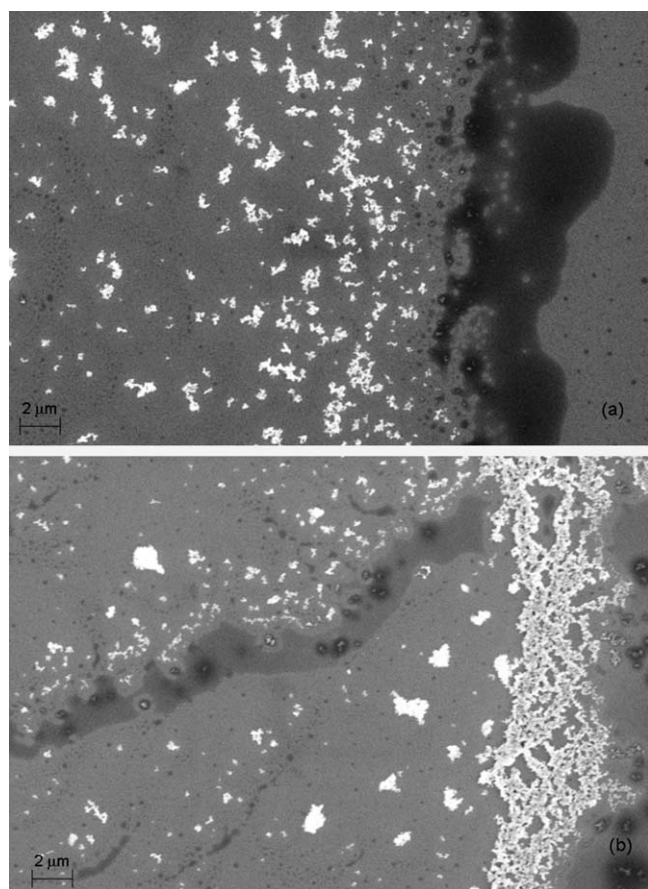


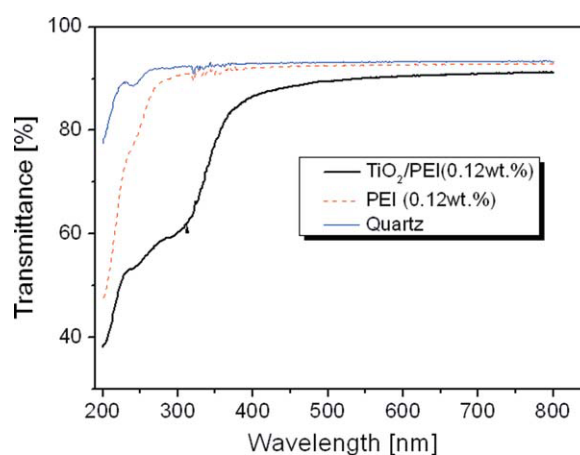
Figure 9 SEM images of TiO₂/PEI (0.12 wt %) printed with an 80% drop overlapping degree at (a) T_{amb} and (b) $T = 50^{\circ}\text{C}$.

After individuating the uniform line condition obtained fixing the drop overlapping at 80%, we studied the effect of temperature on the morphology of the printed TiO₂/PEI (0.03 wt %) and TiO₂/PEI (0.12 wt %) samples. The SEM analysis showed a lower aggregation and a better distribution of nanoparticles in the lines printed at room temperature [Fig. 8(a) and Fig. 9(a)] with respect to the samples printed at $T = 50^{\circ}\text{C}$ [Fig. 8(b) and Fig. 9(b)]. In detail, it was evident that the amount of the material transferred toward the edge of the uniform line

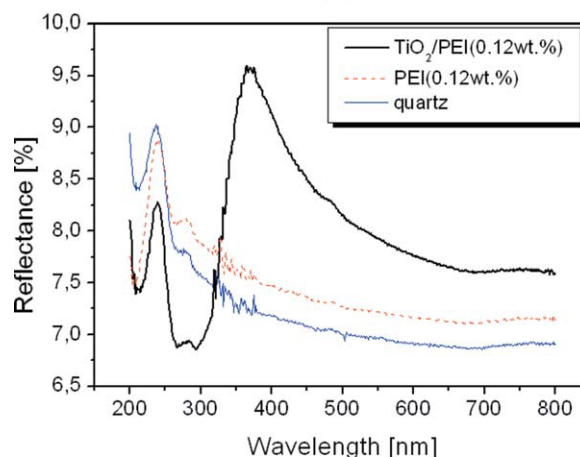
TABLE I
Statistical Analysis of the Size of the TiO₂ Aggregates in the Center of TiO₂/PEI (0.03 wt %) and TiO₂/PEI (0.12 wt %) Lines Printed at T_{amb} and $T = 50^{\circ}\text{C}$

	TiO ₂ aggregate size in TiO ₂ /PEI (0.03 wt %)	TiO ₂ aggregate size in TiO ₂ /PEI (0.12 wt %)
T_{amb}	250 ± 90 nm	290 ± 100 nm
$T = 50^{\circ}\text{C}$	270 ± 100 nm	300 ± 100 nm

increased as the substrate temperature increased because of the coffee-ring effect.^{31,32} A reaggregation process due to the high solvent evaporation rate took place at the edge line, where a continuous structure appeared, differently from the nearly homogeneous distribution of the nanometric aggregates observable in the line center. The size of the TiO₂ aggregates in the line center of the SEM images [Fig. 8(a) and 9(a)] was evaluated by a statistical analysis, and the results are reported in Table I. These results were in agreement with the DLS data and suggest that at the line center, the printing process induced any further aggregation phenomena with respect to the nanoaggregates already present in solution. Moreover, the comparison of the size of the TiO₂/PEI (0.03 wt %) and TiO₂/PEI (0.12 wt %) aggregates of the samples printed at the same temperature and with the same drop overlapping degree suggested an increase of the nanoparticle



(a)



(b)

Figure 10 (a) UV-vis transmittance and (b) reflectance spectra of TiO₂/PEI (0.12 wt %) and PEI (0.12 wt %) films printed on quartz substrates. [Color figure can be viewed in the online issue, which is available at www.interscience.wiley.com.]

dimensions as the PEI concentration increased. Also, this result confirmed the DLS analysis and allowed us to individuate the TiO₂/PEI (0.03 wt %) suspension as the best ink to be processable by IJP.

To investigate the optical properties of the nitrogen-doped TiO₂ nanocomposites, 2 × 2 cm² surfaces were printed on quartz substrates by overlapping single lines. The UV-vis spectra of the TiO₂/PEI (0.12 wt %) and PEI (0.12 wt %) films are shown in Figure 10. Both films had high transmittance (~90%) in the wavelength range 400–800 nm [Fig. 10(a)]. Furthermore, the TiO₂/PEI (0.12 wt %) film had an absorption edge in the range 240–300 nm [Fig. 10(a)] and a reflectance peak centered at 369 nm [Fig. 10(b)] due to the presence of TiO₂ nanoparticles.

CONCLUSIONS

N-doped TiO₂ nanoparticles were dispersed in solution through the use of a polycation polymer (PEI) to manufacture inks for IJP applications. N-TiO₂/PEI/EtOH suspensions at different PEI concentrations were prepared, and a study of the effect of the dispersant content on the ink printability was performed. The suspensions were characterized in terms of viscosity, surface tension, particle size, and time stability. The results of the performed analyses indicated that all of the prepared samples had the right chemico-physical properties for their employment as inks, and in particular, the lower PEI concentration suspension was the preferable one because it was characterized by smaller aggregates. Lines and surfaces of TiO₂/PEI were printed on silicon substrates at different printing parameters (drop emission frequency and overlapping degree, substrate temperature) to define the uniform line conditions. The morphological analysis of the samples showed a lower aggregation and a better distribution of nanoparticles deposited at T_{amb} with respect to the films printed at higher temperatures.

References

- Linsebigler, A. L.; Lu, G.; Yates, J. T. *Chem Rev* 1995, 95, 735.
- Hagfeldt, A.; Gratzel, M. *Acc Chem Res* 2000, 33, 269.
- Huang, S. Y.; Kavan, L.; Exnar, I.; Gratzel, M. *J Electrochem Soc* 1995, 142, L142.
- Gerfin, T.; Gratzel, M.; Walder, L. *Prog Inorg Chem* 1997, 44, 345.
- Lin, H. M.; Keng, C. H.; Tung, C. Y. *Nanostruct Mater* 1995, 6, 1004.
- Park, J.; Lee, J. W.; Kim, D. W.; Park, B. J.; Choi, H. J.; Choi, J. S. *Thin Solid Films* 2009, 518, 588.
- Fujishima, A.; Hashimoto, K.; Watanabe, T. *TiO₂ Photocatalysis: Fundamentals and Applications*; BKC: Tokyo, 1999.
- Aiken, Z. A.; Hyett, G.; Dunnill, C. W.; Wilson, M.; Pratten, J.; Parkin, I. P. *Chem Vapor Deposition* 2010, 16, 19.
- Ko, K. H.; Lee, Y. C.; Jung, Y. J. *J Colloid Interface Sci* 2005, 283, 482.
- Kingon, A. I.; Maria, J. P.; Streiffer, S. K. *Nature* 2000, 406, 1032.
- Le-Clech, P.; Lee, E. K.; Chen, V. *Water Res* 2006, 40, 323.
- Mandzy, N.; Grulke, E.; Druffel, T. *Powder Technol* 2005, 160, 121.
- Asahi, R.; Morikawa, T.; Ohwaki, T.; Aoki, K.; Taga, Y. *Science* 2001, 293, 269.
- Calvert, P. *Chem Mater* 2001, 13, 3299.
- De Gans, B. J.; Duineveld, P. C.; Schubert, U. S. *Adv Mater* 2004, 16, 204.
- Tekin, E.; de Gans, B.-J.; Schubert, U. S. *J Mater Chem* 2004, 14, 2627.
- Service, R. F. *Science* 2004, 304, 675.
- Sato, K.; Li, J. G.; Kamiya, H.; Ishigaki, T. *J Am Ceram Soc* 2008, 91, 2481.
- Tang, F.; Uchikoshi, T.; Ozawa, K.; Sakka, Y. *J Eur Ceram Soc* 2006, 26, 1555.
- Taylor, M. L.; Morris, G. E.; Smart, R. S. C. *Colloids Surf A* 2001, 190, 285.
- Chibowski, S.; Paszkiewicz, M. *J Dispersion Sci Technol* 2001, 22, 281.
- Kitoshi, S.; Ji-Guang, L.; Hidehiro, K.; Takamasa, I. *J Am Ceram Soc* 2008, 91, 2481.
- Peres-Durand, S.; Rouviere, J.; Cuizard, C. *Colloids Surf A* 1995, 098, 251.
- Nussbaumer, R.; Caseri, W. R.; Smith, P.; Tervoort, T. *Macromol Mater Eng* 2003, 1, 288.
- Kim, S. J.; Mckean, D. E. *J Mater Sci Lett* 1998, 17, 141.
- Miyachi, M.; Ikezawa, A.; Tobimatsu, H.; Irie, H.; Hashimoto, K. *Phys Chem Chem Phys* 2004, 6, 865.
- Wang, S. Q. *Coating Process (III)*; Chemical Industry Press: Beijing, 1996.
- Colic, M.; Fuerstenau, D. W. *Powder Technol* 1998, 97, 129.
- Xu, G. L.; Xu, L. N.; Pan, S. L.; Song, G. Z. *Colloids Surf A* 2004, 232, 49.
- Liufu, S. C.; Mao, H. N.; Li, Y. P. *J Colloid Interface Sci* 2005, 281, 155.
- Soltman, D.; Subramanian, V. *Langmuir* 2008, 24, 2224.
- Deegan, R. D.; Bakajin, O.; Dupont, T. F.; Huber, G.; Nagel, S. R.; Witten, T. A. *Nature* 1997, 389, 827.